Journal Of Biomechanics Template

mec46087[1]

[1]Affiliation not available

August 13, 2018

Human Body Models are a powerful design tool for improving engineering with the aim of understanding and preventing injuries to the human body in motor vehicle crashes. Probabilistic injury prediction methods are necessary to account for the variability in the whole population with a reduced number of models. Typically, injury risk curves (IRCs) are used in crash safety to relate the measurements on the model to associated probabilities of injuries. The goal of the current study was to develop injury risk curves for the Femur for the Global Human Body Model Male 50th percentile (GHBM M50) in three-point bending. Therefor, 121 post-mortem human subjects (PHMS) were reconstructed with the GHBM 50 and eight strain (maximum principal strain 95, 99, 100 percentiles and five newly developed metrics) and one stress (maximum principal stress) predictors were measured during simulation. To find the best predictor the IRCs generated for each metric were evaluated based on the following criterion: Goodness of fit, sensitivity, confidence intervals and the influence of outliers. To evaluate the goodness of fit a new method was developed based on the residuals measured between the parametric IRCs and the reference Non-Parametric Maximum Likelihood Estimator. All tested predictors provided an IRC with quality indexes in the recommended range while adding age as a parameter of the IRC always improved significantly the risk prediction. The risks associated with each PMHS tests predicted by all tested metrics were compared. All predictor except one correlate generally well with each other. Based on the results and particularly the Goodness of fit, MPS95 and MPS100 are recommended to predict Femur injuries for the GHBM M50.

Introduction:

In 2015, 5376 pedestrians were killed and 70.000 were injured by car accidents in the US, which is a 9.5 percent increase from 2014. The most common initial point of impact on vehicle is the Front (83,5%) [1]. The most frequent injured body parts are the lower limbs [2].

One powerful tool for improving engineering and prevent potential injuries of the human body in car design alongside Anthropometric Test Devices (ATDs) are Human Body Models (HBMs) [3-4]. HBMs integrate a full representation of the human body incorporating bones, ligaments and internal organs; they are omnidirectional and potentially more biofidelic. While ATDs use global criteria such as moment, force and accelerations for assessing injury risk, HBMs offer the possibility to use local material-based criteria such as stress and strain. The EuroNCAP (ENCAP) already recognized the potential of HBMs, at the IRCOBI conference in 2016, its president, Michiel van Ratingenwrote: “Human body models can complement future assessment strategies to provide a more rigorous and complete evaluation of structure and restraint performance.” [5]. ENCAP already uses HBMs for assessing pedestrian deployable systems [6]. Traditionally, injury prediction with HBMs has been based on the deletion of elements reaching a predefined threshold in stress or strain during the simulation. This method allows a direct visualization of the injuries and accounts

for the effects of structure weakening. However, it does not account for the biomechanical variability and therefore the observed injuries are valid only for the simulated model. It is necessary to introduce a statistical approach to assess the risk for a greater proportion of the population using a reduced set of models [7]. One possibility is to develop Injury Risk Curves (IRCs) like it is currently the state of the art for crash dummies.

A few studies exist for certain parts of the body like the pelvis performed by Peres, Salzar and Leport [7-9] and the ribcage performed by Foman and Mendoz-Vazquez [10-11]. However, to the author´s knowledge, no IRCs have been proposed to predict lower limb fractures in HBMs.

The aim of this study was to develop IRCs to predict the risk of femur fractures in the Global Human Body Model Male 50th percentile(GHBM M50). The data obtained by simulating several Post Mortem Human Subjects (PMHS) experimental tests from the literature were used to develop injury risk curves (IRCs) based on several stress and strain metrics. Furthermore, an evaluation method is proposed and used to determine the best injury predictor.

Material & Method

Tested injury predictors

121 PMHS tests from the literature were simulated with the GHMB M50 model like described in appendix A. The measured moments of fracture were normalized with the formulas described in Appendix B to be able to predict the injury risk not for the specific model but a greater portion of the population. The resulting data were used to test several injury predictors to predict femur fracture, one was the maximum principal stress whereas all others were based on Maximum Principal Strain (MPS). MPS100 is the maximum value of MPS measured on one single element of the femur cortical bone. Because it is believed that this measure can be very sensitive to local strain peak affected by modeling limitations, we also measured MPS99 and MPS95 which are respectively the value of the 99th and 95th percentile of the distribution of MPS for all the elements of the femur. These measures were introduced by Gabler et al. [12]. for measuring strains in the brains and further used in Peres et al. [7] for predicting injuries to the pelvic bone.

These metrics have proven to be less sensitive to modeling artefact when compared to MPS100, however one disadvantage is that they can lead to considering elements which are not adjacent for predicting the same local injury. For example, if the considered structure shows strain concentration at 2 or more different and unrelated locations, MPS95 and MPS99 will treat all elements the same and be calculated over elements from these unrelated locations. This effect is illustrated in the case of a 4-point test bending below where 4 local maximum strain regions are observed at the impactor locations and on the opposite side.

We therefore introduce a new metric which is also based on MPS and considers the average value of MPS for adjacent elements over a predefined search volume Vs. The algorithm will find elements in the structure exhibiting the highest MPS and progressively add adjacent elements until reaching a volume close to Vs. For the list of elements generated using this process, the average (considering element size (Volmean) and element number (mean)) and minimum (Volmin) values were calculated. The procedure is repeated over the first three highest MPS elements found in the structure and the biggest value is kept for Volmin, mean and Volmean.

The predefined volumes defined in this study were one (1571mm3) and five (7853mm3) percent of the femoral shaft volume to allow a better comparison of the results with the MPS 99 and MPS 95. This makes sure that the volume is big enough to minimize the effect of singularities.

Injury Risk Curves (IRC)

All PHMS tests were reconstructed and simulated as described above. All predictors were measured during the simulation on the HBM model for all tests. With this data injury risk curves (IRCs) were generated.

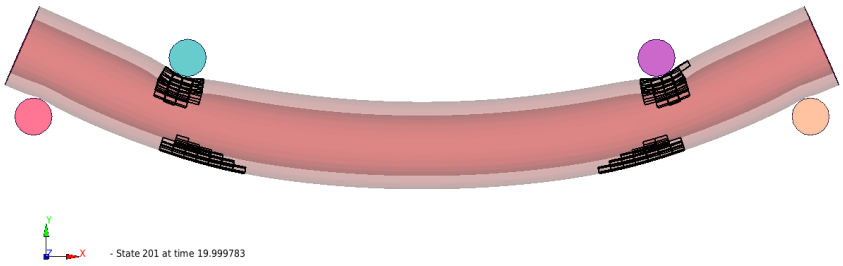

Figure 1: This is a caption

The 12 steps for developing an injury IRC from the ISO/TC22/SC12/WG6 guidelines were followed [13].

The Akaike Information Criteria (AIC) is a frequently used indicator of model fit founded on the information theory. It uses the maximum log likelihood and a penalty term for the number of parameters used in the model. The lower the AIC value the better the fit of the distribution. A survival analysis was performed with the statistical software R to fit the parameters of 3 types of distributions, namely Weibull, loglogistic and lognormal, to the dataset generated for each injury predictor. For each type of distribution, a variant with age adjustment and a variant without were calculated. The AIC value associated with each distribution was determined. Furthermore, QQ plots and the Non-Parametric Maximum Likelihood Estimator (NPMLE) distributions were generated. At last the 95% confidence intervals were calculated and quality indexes of the IRCs were determined for 5%, 20%, and 50% risks of injury as required in the guidelines. The IRCs were proposed for 25, 45, 65 years old and the PHMs average age, which was 57.

These data were used to give a conclusion about the best predictor. Following criteria were used to give a statement, how good a predictor is working for injury prediction: Goodness of fit, Sensitivity, confidence interval and influence of outliers.

To compare the goodness of fit for each predictor the AIC is a common indicator. AIC can be used to compare two models describing the same dependent variable, in our case the same injury predictor. However, it cannot be used to compare models of different dependent variables [14]. Therefore, we used AIC to select the best distribution for a given injury predictor but did not use it to compare the fit between different predictors.

Because there is no existing method in the literature to compare the goodness of fit between two different predictors, a new evaluation method is proposed. The method is based on the calculation of residuals between the calculated injury risk curve and a non-parametric distribution maximizing log likelihood (NPMLE). The NPMLE injury risk curve is characterized by steps. At the middle of each horizontal step i, the distance to the injury risk curve was calculated). Because in every IRC the axis of ordinates shows the risk in percent, no scaling of the data was needed. The resultant residual for each IRC was calculated with this formula:

$Res = \sqrt{(\sum((y_i) - y_i)^2)/n}$

is the risk at the middle of the ith step of the NPMLE and the corresponding risk calculated using the parametric IRC. The resultant residuals for each predictor were compared to assess the predictor best fitting injury data.

For the Sensitivity check a parameter study was performed to evaluate the influence of the mesh size on the

results. A 3-point bending test was simulated with a simplified femur and the mesh size was varied to figure out the influence of elements size on the value of each injury predictor. The predictor values were compared between the smaller and the bigger mesh at 7 levels of bending moment between 100 and 700Nm.

The influence of outliers was estimated using the DFBETAs. DFBETAs are a standard measure of the influence of single data points, they measure the difference in the estimated parameters of a distribution when including or excluding the considered data point. A cutoff value of 0.3 was used to identify overly influential points [13] and the IRCs calculated with and without these data points were compared.

Results:

Analysis MPS data

The MPS100 data generated from the simulated PMHS tests were analyzed. The effect of the following variables on the calculated MPS100 injury limit were evaluated:

-Continous variables: Age, mass, maximal distance to neutral axis (cmax), cross sectional area (csa), Second moment of area about the neutral axis (Ixx), Section modulus (Secmod).

-Categorical variables: Test serie, gender, impact direction, impact velocity, impact location, with or without flesh, with or without axial force.

For continuous variables, correlation plots were generated and the pearson correlation coefficients c as well as p-values between the examined variable and MPS100 were calculated. For categorical variables, box plots were generated and used to conclude if the differences observed in MPS range were significant. The effect of the same variables on the PMHS fracture moment (non-normalized), mfx, was also evaluated. All the graphs, p-vales and pearson correlation coefficients can be found in appendix D.

Age has the strongest correlation to MPS out of all the continuous variables (c= 0.0537, p=5.59E-01), as expected the MPS100 limit decreases with age. A similar relationship is also observed between age and mfx. csa and cmax seem uncorrelated with MPS100 whereas they are strongly correlated with mfx. It is believed that the normalization is the main reason for that as it is aimed at eliminating effects of geometrical differences. If the normalization would work perfectly, we would not expect to observe significant effects of geometry but only of variables correlated to bone properties. Ixx shows a significant correlation with MPS100, however it is much weaker than with mfx suggesting that normalization, though not completely, reduced the effect of Ixx.

Concerning non-categorical variables, we do not see a significant difference in terms of MPS100 between male and female, which would suggest that in our dataset the bone properties were similar between genders. Inclusion of soft tissues around the bone did not influence significantly the MPS100 limit. Variables relative to the impact configuration such as impact velocity, impact location (mid or distal) and impact type (pure bending or combined) did not influence the MPS100 values significantly. For impact direction, we observe a significant difference between PA and ML impacts, which cannot be explained. When looking at the different impact test series, only Forman 2012 presents significantly higher MPS100 values when compared to Funk 2004, Ivarsson 2009, Kennedy 2004 and Kerrigan 2004. This difference is due to the young age of the PMHS tested in this test serie in comparison with the others. Generally, and as it would be expected, MPS100 show little correlation with geometrical variables and little dependence to the loading conditions. Age is the variable which seems to have the most predictive ability for the MPS100 limit which is consistent with the known effect of age on bone quality.

IRC

Figure 2 shows the different graphs generated for each predictor presented by the example of MPS95. Figure 2.1 shows the IRC for the log logistic distribution and the associated 95 percentile confidence intervals. Confidence intervals were very narrow for all tested predictors and distributions. In 2.2 the influence of the critical DFBETAS is checked, the black IRC is calculated with all PMHS tests included, the green and blue curves show the change in the IRC when excluding PMHS tests with a DFBETA superior to 0.3 in the calculation of the scale and location parameters of the log-logistic distribution. There is no big difference between these IRCs. 2.3 shows QQ plot between the PMHS data and the loglogistic parametric distribution. In 2.4 the loglogistic distribution is shown together with the NPMLE and the Loglikelihood, AIC and BIC are shown for this distribution.

	AIC baseline	AIC age	QI at 5%	QI at 25%	QI at 50%	DFBETAs	Resultant residual
Stress (Weibull)	-483.21	-504.53	0.16	0.09	0.06	2	0.00644
MPS95	-1018.53	-1041.20	0.22	0.14	0.12	2	0.00159
MPS99	-923.84	-950.95	0.23	0.15	0.12	3	0.00221
MPS100	-856.96	-886.51	0.24	0.16	0.14	3	0.00218
Vol_1571_mean	-915.82	-943.52	0.25	0.15	0.14	4	0.00251
Vol_1571_volmean	-913.56	-941.18	0.23	0.15	0.14	4	0.00250
Vol_7853_mean	-994.93	-1020.75	0.22	0.15	0.14	4	0.00242
Vol_7853_volmean	-995.85	-1023.32	0.21	0.14	0.14	4	0.00245
Vol_7853_min	-1362.60	-1362.69	0.20	0.13	0.15	6	0.00473

Table nr. 1 shows the AIC for age-adjustedand non-age adjusted distributions, the Quality Index (QI), the number of DFBETAs and the Residuals for every predictor. For all predictor and distributions, the AIC for age-adjusted distributions are lower than for non-age adjusted distributions. Furthermore, for stress the AIC is lower by a Weibull distribution while for strain predictors, the loglogistic distribution leads to lower AIC values. also, the Quality Index (QI) at 5 %, 25 % and 50% risk are determined. The range of all QIs is from 0.06 to 0.25. The values of the resultant residual differ from 0.00159 (MPS95) to 0.00644 (stress). The smaller the value, the better the goodness of fit of the IRC to the NPMLE. This result is consistent with the optical comparison of the created graphs. The parameters of the best distributions for each tested predictor are given in appendix E.

As explained in the methods, the sensitivity of the predictors to mesh size was evaluated using a simplified femur geometry impacted in a standard 3-point bending configuration, 2 mesh sizes were tested, xxx mm and yyy mm.[CM1] The values of each predictor were measured at 7 levels of bending moment between 100 and 700Nm. The discrepancy in the results observed for each predictor between the 2 mesh sizes were evaluated, the predictor exhibiting the smaller discrepancy being considered less sensitive to mesh size. Looking at the results MPS100, MPS99 and MPS95 exhibit smaller mesh size discrepancies (0.3-18.6%) when compared to all volumic based metrics (3.8-40.3%). However, no clear trend is observed otherwise, different predictors exhibiting the least amount of discrepancy at different levels of bending moment.

Discussion

General discussion on the IRCs

Figure nr. 3 shows that the risk for a given stress value is higher for 65 years old (orange) as for 45years old (blue), the same is observed for all predictors. For all predictors, the width of the confidence intervals is small, QI are all below 0.5 which is considered good according to the ISO/TC22/SC12/WG6 recommendations [13]. The influence of singular data point is negligible as confirmed by the lack of effect observed when excluding the outliers according to DFBETA values. For all strain predictors, the loglogistic distribution with age adjustment was the best fit according to the AIC value. The associated IRCs follow generally well the NPMLE indicating that the parametric distributions fit the PMHS data well which is confirmed when looking at the QQ plots. The IRCs for the strain metrics are particularly accurate up to 80-85% of risk, more discrepancy with the NPMLE being observed for higher risk values. For the stress IRC, the Weibull distribution with age adjustment exhibited the best AIC value. The Weibull IRC does not fit the NPMLE distribution as well as it is the case for the strain predictors. The NPMLE shows a change of curvature around 150 MPa which is consistent with the yield stress defined in the GHBM. It is believed that this change in IRC curvature is due to the material behavior changing from elastic to plastic in the model.

As explained previously it is not possible to compare the AIC value between different predictors. To the author´s knowledge, no method has so far been proposed to achieve this. Therefor the Residual for each step of the NPMLE was calculated. The resultant residual represents the goodness of fit of the IRC. The results are consistent with the optical evaluation of the graphs. This method delivers reliable results up to a risk of 80-85%. Above this level the distance between the NPMLE are getting bigger so one residual must cover a bigger area. Because of that, the difference between the NPLME and the parametric IRC from a level over 80% risk is underrepresented in the calculation. However, this underrepresentation can be seen in the IRC for every predictor, so it is estimated that the residuals are still comparable.

Which metric is best predicting injuries?

If we compare all predictors, MPS95 is the best in terms of goodness of fit according to the resultant residuals´ value whereas stress is the worst. In terms of the quality index, not much difference is observed between all strain predictors but stress QIs are lower than strain predictors´ QIs. As described before, influential points do not change significantly the injury risk curves for any of the tested predictors. As presented in the results it was not possible to conclude on the sensitivity to the mesh of the tested predictors. Considering these results, MPS95 seems to be a good candidate to predict femur fracture in the GHBM M50 model being the best in terms of goodness of fit and the second in terms of QIs.

The risk associated to each PMHS test was calculated for each predictor based on the previously developed age adjusted injury risk curves and the predictor value measured in the corresponding simulation. Then linear regressions between each predictors were calculated. Table nr. 2 shows R2 for all predictors. Vol7853min is not correlating with any of the other injury predictors with a maximum R2 of 0.301. All other strain metrics correlate very well with one another, R2 are between 0.928 and 0.997. When looking at all Volume based metrics other than Vol7853_min, they are essentially predicting the same risks for all PMHS tests with R2 superiors to 0.992 and regression slope coefficients between 0.994 and 0.998. R2 values are slightly lower between MPSxx metrics and volumetric ones but still high (>0.970) and the regression slope coefficients are very close to 1. MPS95 shows a bit less correlation with MPS100 with a R2 of 0.928. Stress is correlating fairly well with all strain predictors (R2>0.903) except with Vol7853_min. Overall all metrics except Vol7853-min predict similar risk levels for the PMHS tests used to develop the IRCs which would be expected. Outside of Vol7853_min, stress is the metric showing the most difference with all others. MPS95 differs also slightly from MPS100 but much less from other strain metrics. Given that MPS95 has shown to be the best injury predictor in terms of goodness of fit, we recommend using MPS95 or the strain metrics which best correlate to it: MPS99, Vol1571_mean, Vol1571_volmean, Vol7853_mean and Vol7853_volmean. To confirm these results, simulating load cases outside of the ones used to develop the IRCs would be necessary.

	stress	MPS95	MPS99	MPS100	Vol:1571 mean	Vol:1571 volmean	Vol:7853 mean	Vol7853 volmean	Vo mi
stress	1	0.903	0.937	0.927	0.929	0.922	0.914	0.920	0.2

MPS95	0.903	1	0.979	0.928	0.973	0.970	0.985	0.973	0.3
MPS99	0.937	0.979	1	0.978	0.998	0.993	0.991	0.994	0.2
MPS100	0.927	0.928	0.978	1	0.979	0.970	0.953	0.970	0.2
Vol1571_mean	0.929	0.973	0.998	0.978	1	0.997	0.993	0.997	0.2
Vol1571_volmean	0.922	0.970	0.993	0.970	0.997	1	0.992	0.995	0.2
Vol7853_mean	0.914	0.985	0.991	0.953	0.993	0.992	1	0.994	0.3
Vol7853_volmean	0.920	0.973	0.994	0.970	0.997	0.995	0.994	1	0.2
Vol7853_min	0.219	0.304	0.257	0.205	0.261	0.266	0.301	0.286	1

Table nr. 2

Comparison with data from literature

Subit et al. 2013 [15] reports results from femur cortical bone tensile tests performed on femur samples from 4 subjects, 2 of which were young adults (37 and 40 years old) and the 2 others elderly (72 and 75 years old). Ultimate strains at failure for young adults were 0.86 and 0.67% in dynamic condition and 0.99% in static conditions. For elderlies, ultimate strains were 0.66 and 0.64% in dynamic, 0.92 for both in static. Using the log-logistic age adjusted injury risk curve developed for MPS100 with an age of 38.5 years old, we get a 50% risk at a value of approx. *2.0* % which higher than the Subit et al. reported values for young adults. Using an age of 73.5 years old 50% risk is obtained for a MPS value of approx. 1,0% which would be consistent with the values reported by Subit et al. 2013 for elderly. Yamada [16] reports ultimate tensile strain values of 1.41% for wet bones and 1.24% for air-dried bones for adults aged 20 to 39 years old. Using an age of 30-year-old with the MPS100 IRC, we find 50% risk to be at a value of approx. 2.2% which is higher than the Yamada reported values. Hansen et al 2008 [17] tested several samples taken from 1 male aged 51 years old. Tensile tests were conducted at velocities ranging from 0.1 to 18 strain/s and ultimate strain vs strain rate data were fitted using a negative exponential regression. Using this regression, ultimate strain values of 2.75% at 0.1 strain/s and 1% from 10 strain/s to 18 strain/s were reported showing the strong rate dependency of the femur cortical bone. Using an age of 51, we find a 50% risk at a value of approx. 1.8% MPS100 between the Hansen reported values for static and dynamic loading. Overall, the IRC predicted MPS100 limits are superior to the ones reported in 2 literature reported values (Yamada 1970 and Subit 2013) and in agreement with the ones reported in another (Hansen 2008).

Limitations

An important point is that nearly solely simple tree-point bending tests were simulated. Only Ivarsson had a test setup that investigates the influence of axial compression on the behavior of the bone during a 3-point bending test. This depicts the loads of a pedestrian more realistically during an accident, because of the loads on the bone due to gravity. Nevertheless, the axial compression differs from 4kN up to 16kN, which is higher than the expected load to depict the bodyweight. In the simulations, the impactor was rigid, but a bonnet is designed of a plastically deformable material to absorb forces during an impact to protect the occupant. In general, it is questionable if the IRCs developed in this study which are based on very simplified loading conditions will still be valid when applied to the much more complex scenarios expected in pedestrian impacts.

In addition, there are still some limitations for the reliability of the generated IRCs with this dataset. The fracture moments were normalized for each cadaver using assumptions of the beam theory. However, the cases simulated including complex geometries, dynamic loadings elastoplastic material properties are not covered by the traditional beam theory. If the normalization method has been validated in this study, some doubts remain as to the extent of the error generated by oversimplification of the assumptions made during normalization compared to the variability of the PMHS. More work would be necessary to whether validate further the use of simple assumptions or develop more refined normalization methods.

All tested predictors in this study were homogeneous, isotropic and did not consider loading rate, which might not be sufficient to account for the complexity of the real bone mechanical behavior. It is known that

bone material properties are significantly different in the collagen fiber direction, especially in the case of long bones we observe stronger behavior in the longitudinal direction, this is not considered in the predictors tested in this study. Moreover, it is known that strain rate influences the fracture limits of the bones in terms of maximum stress and strain, none of the tested predictors integrates the effect of loading rate.

Caution is advised in the use of the IRCs for high risk levels because as larger discrepancies with the NPMLE were observed in this region for the strain metrics.

Conclusions:

All tested predictors led to good IRCs, particularly the IRCs were reasonably matching the Non-Parametric Maximum Likelihood Estimator, the confidence intervals were all good according the ISO/TC22/SC12/WG6 recommendations and the influence of individual data point was negligible. Additionally, including age as a parameter in the IRC systematically led to improvements in the AIC value. Some predictors exhibited significantly better fit and others were more sensitive to mesh size. Considering all evaluation criterion, we recommend the use of MPS95 to predict femur fractures with the GHBM M50 in bending conditions including when axial force is present. However, to come with a definitive conclusion on the validity of the developed IRCs, it would be necessary to test their predictive capability using additional tests independent of the data used in this study. More complex loading conditions could be simulated, possibly accident reconstructions.

References:

[1] U.S. Department of Transportation National Highway Traffic Safety Administration. (2018, 03). Traffic Safety Facts [PDF document]. Retrieved from https://crashstats.nhtsa.dot.gov/#/PublicationList/36 on 10.08.2018.

[2] Martin JL., Lardy A., Laumon B. (2011). Pedestrian Injury Patterns According to Car and Casualty Characteristics in France. *Ann Adv Automot Med*, 55, pp. 137–146.

[3] Combest J. (2016, 10). Current Status and Future Plans of the GHBMC (Global Human Body Models Consortium) [PDF document]. Retrieved from http://www.ghbmc.com/wp-content/uploads/2016/10/HuMo16_15_Combest_G on 10.08.2018.

[4] Fressmann D. (2012, 10). Vehicle Safety using the THUMSTM Human Model [PDF document]. Retrieved from https://www.dynamore.de/de/download/papers/ls-dyna-forum-2012/documents/passive-3-2 on 10.08.2018.

[5] van Ratingen M. (2016). Saving Lives with Safer Cars: The Past, Present and Future of Consumer Safety Ratings. *IRCOBI Conference*, IRC-16-01, pp 1-17.

[6] European New Car Assessment Programme. (2017). Technical Bulletin Pedestrian Human Model Certification Version 1.0 [PDF document]. Retrieved from https://cdn.euroncap.com/media/32277/tb-024-pedestrian-human-model-certification-v10.pdf on 19.07.2018

[7] Peres J., Auer S., Praxl N. (2016). Development and comparison of different injury risk functions predicting pelvic fractures in side impact for a Human Body Model. *IRCOBI Conference*, IRC-16-87, pp 661-678.

[8] Salzar R., Genovese D. (2009). Load path distribution within the pelvic structure under lateral loading. *Int J. Crashworthiness*, Vol. 14(1), pp. 99-110.

[9] Leport T., Baudrit P. (2007). Assessment of the pubic force as a pelvic injury criterion in side impact. *Stapp Car Crash Journal*, Vol. 51, pp.467–88.

[10] Forman JL. and Kent RW. (2012). Predicting Rib Fracture Risk with Whole-Body Finite Element Models: Development and Preliminary Evaluation of a Probabilistic Analytical Framework. *Ann Adv Automot Med.,* Vol. 56, pp. 109–124.

[11] Mendoza-Vazquez M., Davidsson J., Brolin K. (2015). Construction and evaluation of thoracic injury risk curves for a finite element human body model in frontal car crashes. *Accident Analysis & Prevention,* Vol. 85, pp. 73-82.

[12] Gabler LF., Crandall JR., Panzer MB. (2016). Assessment of Kinematic Brain Injury Metrics for Predicting Strain Responses in Diverse Automotive Impact Conditions. *Annals of Biomedical Engineering*, Vol. 44, Issue 12, pp. 3705–3718.

[13] Petitjean A., et al. (2015). 26.3.3 Recommendations for Development of Injury Risk Curves. In Narayan Yoganandan (Eds.), Accidental Injury Biomechanics and Prevention Third Edition (pp. 782-787). New York Heidelberg, Dordrecht London: Springer.

[14] Posada D., Buckley TR. (2004). Model Selection and Model Averaging in Phylogenetics: Advantages of Akaike Information Criterion and Bayesian Approaches Over Likelihood Ratio Tests. *Systematic Biology*, Vol. 53, Issue 5, pp. 793–808.

[15] Subit D, Arregui C., Salzar R., Crandall J. (2013). Pediatric, Adult and Elderly Bone Material Properties. *IRCOBI Conference,* IRC-13-87, pp. 760-768.

[16] Yamada H., Evans FG. (1970). 3.1.1.1. Tensile Properties of Compact Bone. In H. Yamada (Eds), Strength of Biological Materials (pp. 19-35)

[17] Hansen U., et. al. (2008). The Effect of Strain Rate on the Mechanical Properties of Human Cortical Bone. *Journal of Biomechanical Engineering*, Vol. 130, Issue 1.

Appendix A: How the data were generated:

1. Research

Kennedy et al. [A.1]

Lateral to medial (25 PHMS) and posterior to anterior (20 PHMS) loading direction were tested with a 3-point bending test. The surrounding tissue wasn't removed. The impactor (9.8kg, Ø=35mm) "was dropped from a height of 2.17m" [Kennedy page 7]. This led to an impactor velocity of 5m/s.

Kerrigan 2003 et al. [A.2]

In this study, only the lateral-medial direction was tested in a 3-point bending test with 4 matched pairs of femur. The tests employed "one test for reliability, two tests for differences in load location (impactor was positioned distal or proximal) and one for the effect of the flesh). The impactor velocity was 1.2 m/s and the impactor diameter was $\frac{1}{2}$" (12.7 mm).

Kerrigan 2004 et al. [A.3]

Twelve leg specimens were ramped to failure with an impactor. "Half of the specimens (6) were loaded at the mid shaft and the other half were loaded at a location on third the length of the distal end" [Kerrigan 2004]. There were no exact data for the impactor given. But in the study of Forman et al, the author refers to the paper of Kerrigan, because the "preparation and testing methods" [Forman et al. page 525] were the same. So, the assumption was made, that the impactor velocity and geometry were like they have been described by Forman (v=1.5m/s, Ø=13mm).

Forman et al. [A.4]

Forman performed a 3-point bending test with 16 adult specimens in lateral-medial loading direction. The tissue was removed and the impactor (v=1.5m/s, Ø=13mm) was surrounded by a foam. Because there were no data about the foam, in the simulation the foam from the Ivarsson study was used.

Funk et al. [A.5]

15 femurs without surrounding tissue were ramped to failure by an impactor (v=1.2m/s, Ø=12mm). Lateral-medial (7) and posterior-anterior (8) loading directions were tested.

Ivarsson et al. [A.6]

The [...] study aims to evaluate the dependence of femoral shaft fracture on combined axial compression and applied bending [...]. [Ivarsson 253] Therefor, 29 dynamic combined and 10 three-point bending tests were made. The foam padded Impactor (Ø=25.4mm, v=1.5m/s) ramped the specimens till failure. The foam was modeled based on the "viscoelastic properties of the foam padding material" [Ivarsson 276] that was given in the Appendix. In the compression tests an axial compression of 4, 8, 12 or 16kN was brought on the specimens and was hold during the 3-point bending tests.

2. Description of the PMHS test series

Several studies focused on estimating the response of the human femur to 3-point bending, a detailed description of the test setups used in this study can be found in appendix xxx.

Author	Year	Axial force	Velocity [m/s]	Impactor Diameter [mm]	Impactor location	Impact direction	Soft tissues	foam
LM	PA	Yes	No					
Kennedy	2004	none	5	35	mid	25	20	45
Kerrigan	2003	none	1.2	12.7	dist:3, mid:4	8	0	1
Kerrigan	2004	none	1.5	13	dist:6, mid:6	12	0	12
Forman	2012	none	1.5	13	mid	16	0	0
Funk	2004	none	1.2	12	mid	7	8	0
Ivarsson	2009	yes	1.5	25.4	mid	0	39	0

Table nr 1 gives a summary of the test conditions used in each study. For most test series, the impact occurred at the mid femur, some in the Latero-Medial (LM) and others in a Posterior-Anterior (PA) direction. In Kennedy 2004 and Kerrigan 2003 and 2004, the tested femur was recovered with the surrounding soft tissues whereas soft tissues were removed in Forman 2012, Funk 2004 and Ivarsson 2009. Axial forces ranging from 4 to 16 kN were applied in Ivarsson 2009. Impact velocities range from 1.2 to 5m/s and in some tests a foam was placed between the femur and the impactor. Overall 121 3-points bending tests were selected and simulated with the HBM, PMHS average age was 57.

3. Simulation

All simulations were performed using LS_DYNA (Version 7.1.2, Livermore Software Technology Corporation, Livermore). For all study simulations the same test setup was used expect Ivarsson. At first, the right femurs of GHBM M50 v.4.5 was isolated from the whole model with and without the surrounding

tissue. Element deletion was turned off to allow a proper measurement of the strains. Then the femur was positioned in the pottings, modeled as rigid and using the geometry described in the published papers. The femur was fixed to the potting using the option *CONSTRAINED_EXTRA_NODES. Then the rigid impactor was positioned in the middle of the diaphysis or in the distal position. The Roller with the pottings on top were supported by a rigid plate, the contact force between them being monitored during the simulation. The contacts both between femur and impactor and plate and roller were modeled with the *AUTOMATIC_SURFACE_TO_SURFACE option (contact thickness = 1mm) using an edge to edge detection and a static friction coefficient of 0.1 and a dynamic friction coefficient of 0.15 At last, an initial or constant velocity was imposed on the impactor using options *INITIAL_VELOCITY_RIGID_BODY or *BOUNDARY_PRESCRIBED_MOTION respectively. The resulting forces measured in the simulations were filtered using the same filter as described in the respective papers. For some simulations, a foam was placed between impactor and femur according to the described test conditions. The foam material properties were represented using MAT_163: MODIFIED_CRUSHABLE_FOAM and stress strain properties from Ivarssons study.

For the Ivarsson combined studies, the test setup was slightly different. The pottings could slide along the simulated floor. During the first ten milliseconds of the simulation the desired axial force was progressively applied and maintained the whole simulation time. Then the impactor displacement started resulting in the 3-point bending test.

Appendix B: Normalization technique

Datasets of biomechanical tests commonly contain PMHS with characteristics (e.g. height, mass, bone/soft tissue behavior, etc.) different from an average male. It is therefore not correct to correlate directly the injury outcome of these PMHS to the response of a 50th percentile surrogate, whether it is a dummy or a HBM. Normalizing techniques have been developed to enable the use of PMHS tests performed with PMHS of different sizes than the surrogate [16-17]. [CM2] In our case, normalizing consists in achieving an equivalent severity level between a given PMHS test and the corresponding simulation. Traditionally severity for biological tissues is understood as the maximum stress. The stress level experienced by the PMHS at failure can be estimated using the beam theory and the fracture moment observed in the experiment. Knowing geometrical characteristics of the Femur of the PMHS and the simulation model such as the area moment of Inertia and the maximum distance to neutral axis it is possible to calculate an equivalent fracture moment corresponding to the same level of stress for the simulation as for the PMHS using equation 1.

Where MPMHS, cPMHS and IPMHS are the bending moment, maximal distance to neutral axis and moment of inertia of the PMHS and MModel, cModel and IModel are the moment, maximal distance to neutral axis and moment of inertia of the Model. For the combined tests the axial force to be applied during the simulation was calculated by this equation:

PPMHS and APMHS are the axial compression force and cross-sectional area of the PMHS and PModel and AModel the axial force and cross-sectional area of the model. The calculated compression for every PHMS was imposed during the simulation for Ivarsson 2009.

The strain levels at fracture for the simulation of a given PMHS test were measured at the time when the bending moment reached the calculated equivalent fracture moment for the model (equation 1). To validate the normalization procedure, each PMHS test was simulated with the GHBM Male 50th (M50) and 95th (M95) percentile. Results were normalized to the corresponding Model dimension using the previously described method. For the M95 model, the strains were also measured without normalizing (using the PMHS fracture moment directly). The correlation of the nominal (non-normalized) and normalized M95 strains with the M50 model strains were analyzed to conclude on the benefit of normalizing.

For checking the efficiency of the normalizing method, the correlation between the predictor values from the M50 and the M95 simulations normalized and non-normalized were studied. Graph x and x show respectively the M95 non-normalized and normalized stress values against the M50 normalized stress values, perfect 1 to 1 correlation is represented by the blue line. It can be observed that in the case of the normalized M95 data, the linear fit is much closer to the perfect correlation indicating a positive effect of scaling which is equally observed for MPS95 on figure x and x. Globally, normalization improve the correlation between M50 and M95 values for all predictors. The linear fit is the closest to the perfect fit in the case of the normalized stress whereas for the strain metrics, the normalized M95 values are systematically higher than the M50 ones, the difference being attenuated when going from MPS100 to MPS95. Considering the results described, it is concluded that the normalization method is valid and can be used to correlate the results of the M50 simulations to the injury outcome of the different PMHS tests.

Appendix C: Table of all reconstructed PMHS tests:

PMHS number	age	gender	ixx	cmax	Direction	Location	type	mfx	F axial	F axial normalized
kennedy2006 1	41	F	25630	19.22	LM	mid	bend	335	none	none
kennedy2006 2	45	M	21620	16.42	LM	mid	bend	318	none	none
kennedy2004 3	49	M	41070	20.03	LM	mid	bend	443	none	none
kennedy2006 4	42	M	46950	19.43	LM	mid	bend	541	none	none
kennedy2005 5	49	F	14200	13.17	LM	mid	bend	272	none	none
kennedy2008 6	43	M	38840	16.36	LM	mid	bend	428	none	none
kennedy2007 7	41	F	13550	12.77	LM	mid	bend	258	none	none
kennedy2006 8	47	F	16890	16.36	LM	mid	bend	280	none	none
kennedy2006 9	45	M	28950	14.96	LM	mid	bend	434	none	none
kennedy2007 10	43	F	20520	16.76	LM	mid	bend	281	none	none
kennedy2006 11	44	M	27580	18.95	LM	mid	bend	396	none	none
kennedy2006 12	41	F	13730	12.75	LM	mid	bend	249	none	none
kennedy2006 13	42	M	40260	17.96	LM	mid	bend	443	none	none
kennedy2007 14	41	M	19940	16.16	LM	mid	bend	322	none	none
kennedy2006 15	41	M	52200	18.35	LM	mid	bend	279	none	none
kennedy2006 16	41	M	26480	16.76	LM	mid	bend	410	none	none

kennedy20064 17	M	42110	16.76	LM	mid	bend	496	none	none
kennedy20078 18	M	26890	16.56	LM	mid	bend	349	none	none
kennedy20061 19	F	12600	12.97	LM	mid	bend	231	none	none
kennedy20062 20	M	38090	18.35	LM	mid	bend	414	none	none
kennedy20061 21	M	50940	17.04	LM	mid	bend	368	none	none
kennedy20061 22	M	27800	16.16	LM	mid	bend	357	none	none
kennedy20072 23	F	12930	15.96	LM	mid	bend	267	none	none
kennedy20067 24	F	19200	14.36	LM	mid	bend	333	none	none
kennedy20067 25	F	17370	15.16	LM	mid	bend	296	none	none
kennedy20065 26	M	26360	14.42	PA	mid	bend	298	none	none
kennedy20061 27	F	39710	18.82	PA	mid	bend	373	none	none
kennedy20069 28	M	56130	16.42	PA	mid	bend	447	none	none
kennedy20068 29	F	28700	15.22	PA	mid	bend	334	none	none
kennedy20062 30	M	65870	19.43	PA	mid	bend	564	none	none
kennedy20079 31	F	16420	12.77	PA	mid	bend	252	none	none
kennedy20063 32	M	37480	16.16	PA	mid	bend	429	none	none
kennedy20070 33	F	23550	12.57	PA	mid	bend	308	none	none
kennedy20071 34	F	14720	12.77	PA	mid	bend	222	none	none
kennedy20066 35	M	39010	16.82	PA	mid	bend	399	none	none
kennedy20067 36	F	23770	12.97	PA	mid	bend	334	none	none
kennedy20065 37	M	28510	15.76	PA	mid	bend	373	none	none
kennedy20070 38	F	20890	12.17	PA	mid	bend	271	none	none
kennedy20074 39	M	21110	14.16	PA	mid	bend	221	none	none
kennedy20071 40	F	22190	13.97	PA	mid	bend	267	none	none
kennedy20068 41	M	45080	16.16	PA	mid	bend	412	none	none

kennedy2006-42	69	M	40090	16.56	PA	mid	bend	438	none	none
kennedy2006-43	64	M	44420	16.16	PA	mid	bend	456	none	none
kennedy2007-44	74	F	23670	13.57	PA	mid	bend	371	none	none
kennedy2007-45	73	F	15360	13.77	PA	mid	bend	184	none	none
kerrigan2006-1	66	M	30019	14.51	LM	mid	bend	548	none	none
kerrigan2006-2	69	M	57118	18.06	LM	mid	bend	568	none	none
kerrigan2006-3	65	M	30934	13.19	LM	mid	bend	640	none	none
kerrigan2007-4	74	M	31274	13.71	LM	mid	bend	424	none	none
kerrigan2006-5	69	M	34179	14.17	LM	mid	bend	488	none	none
kerrigan2007-6	74	M	39543	15.5	LM	mid	bend	685	none	none
kerrigan2007-7	71	M	27028	14.27	LM	dist	bend	394	none	none
kerrigan2007-8	78	M	38651	16.69	LM	dist	bend	411	none	none
kerrigan2007-9	74	M	56556	18.6	LM	dist	bend	599	none	none
kerrigan2007-10	74	M	39270	18.91	LM	dist	bend	465	none	none
kerrigan2007-11	77	M	18060	11.78	LM	dist	bend	380	none	none
kerrigan2007-12	77	M	39285	18.21	LM	dist	bend	466	none	none
funk2004-1	67	M	66518	16.5	PA	mid	bend	355	none	none
funk2004-2	59	M	70771	14.7	PA	mid	bend	593	none	none
funk2004-3	40	M	49508	15.4	PA	mid	bend	605	none	none
funk2004-4	55	M	21297	14	PA	mid	bend	363	none	none
funk2004-5	70	M	33845	13.2	PA	mid	bend	359	none	none
funk2004-6	69	M	38264	13.7	PA	mid	bend	460	none	none
funk2004-7	51	M	45506	17.1	PA	mid	bend	599	none	none
funk2004-8	66	M	22908	14.5	PA	mid	bend	373	none	none
funk2004-9	67	M	35234	14	LM	mid	bend	435	none	none

funk2004-10	59	M	42940	16.7	LM	mid	bend	497	none	none
funk2004-11	40	M	26634	15.2	LM	mid	bend	528	none	none
funk2004-12	55	M	27008	14	LM	mid	bend	389	none	none
funk2004-13	70	M	23189	14.3	LM	mid	bend	356	none	none
funk2004-14	69	M	32075	10.5	LM	mid	bend	419	none	none
funk2004-15	51	M	39568	14.4	LM	mid	bend	543	none	none
kerrigan2005-1	35	M	29727	13.6	LM	mid	bend	635	none	none
kerrigan2005-5	39	F	24661	13.8	LM	mid	bend	362	none	none
kerrigan2005-6	34	F	27292	15.9	LM	mid	bend	340	none	none
kerrigan2005-7	34	F	28545	14.7	LM	mid	bend flesh	377	none	none
forman2013-1	36	M	27605	15.3	LM	mid	bend	283	none	none
forman2013-2	20	M	28247	14.9	LM	mid	bend	533	none	none
forman2013-3	27	M	28397	13.9	LM	mid	bend	522	none	none
forman2013-4	43	M	27661	15.2	LM	mid	bend	579	none	none
forman2013-5	35	M	23576	14.1	LM	mid	bend	409	none	none
forman2013-6	57	F	12534	12.2	LM	mid	bend	287	none	none
forman2013-7	19	M	28314	14.5	LM	mid	bend	528	none	none
forman2013-8	52	M	29886	14.6	LM	mid	bend	602	none	none
forman2013-9	27	M	32765	15.3	LM	mid	bend	587	none	none
forman2013-10	42	M	29591	14.7	LM	mid	bend	577	none	none
forman2013-11	25	M	14671	12.3	LM	mid	bend	297	none	none
forman2013-12	28	M	27222	14.5	LM	mid	bend	567	none	none
forman2013-13	35	M	21476	13.4	LM	mid	bend	407	none	none
forman2013-14	36	M	34652	14.9	LM	mid	bend	675	none	none
forman2013-15	28	M	28578	15.1	LM	mid	bend	577	none	none

forman201319 16	M	26625	14.2	LM	mid	bend	512	none	none
ivarsson200951 1	M	35036	15.7	PA	mid	comb	413	11115	11963
ivarsson200951 2	M	42201	12.9	PA	mid	comb	213	14700	13898
ivarsson200902 3	M	39980	15.4	PA	mid	comb	293	3075	2903
ivarsson200902 4	M	46038	15.8	PA	mid	comb	494	13700	11771
ivarsson200902 5	M	38404	13	PA	mid	comb	393	3225	3176
ivarsson200902 6	M	39484	15.8	PA	mid	comb	532	3947	4076
ivarsson200949 7	M	44624	15.8	PA	mid	comb	437	6667	6290
ivarsson200949 8	M	40234	14.1	PA	mid	comb	604	12030	12013
ivarsson200902 9	M	36685	15.4	PA	mid	comb	490	3640	4071
ivarsson200944 10	M	31759	15.1	PA	mid	comb	480	14700	16142
ivarsson200944 11	M	31206	15.6	PA	mid	comb	513	6780	7541
ivarsson200958 12	M	58209	17.7	AP	mid	comb	743	3292	2517
ivarsson200958 13	M	59000	17.4	AP	mid	comb	744	7400	6040
ivarsson200905 14	M	24971	14.9	AP	mid	comb	420	7427	9264
ivarsson200905 15	M	22660	13.9	PA	mid	comb	276	14115	17842
ivarsson200953 16	M	29600	14.2	AP	mid	comb	475	11756	12187
ivarsson200953 17	M	27630	14.1	AP	mid	comb	487	6844	7675
ivarsson200904 18	F	20356	14.1	AP	mid	comb	353	6405	8517
ivarsson200904 19	F	21264	13.9	PA	mid	comb	170	12125	16367
ivarsson200940 20	F	19727	13.6	PA	mid	comb	342	6710	10595
ivarsson200940 21	F	17322	13.9	AP	mid	comb	424	10980	17971
ivarsson200945 22	F	19794	13.4	AP	mid	comb	317	2400	2968
ivarsson200945 23	F	20063	13.4	AP	mid	comb	282	7300	8864
ivarsson200900 24	F	16791	12.3	AP	mid	comb	269	12000	16105

ivarsson20050 25	F	26270	14.2	AP	mid	comb	468	6920	7484
ivarsson20050 26	F	21276	14.7	AP	mid	comb	442	2800	3148
ivarsson20056 27	F	13517	12.8	AP	mid	comb	282	12475	22208
ivarsson20062 28	M	32914	15	PA	mid	comb	180	11800	12529
ivarsson20052 29	F	17069	12.4	PA	mid	bend	120	none	none
ivarsson20052 30	F	19103	16.7	AP	mid	bend	147	none	none
ivarsson20063 31	M	38372	15.9	AP	mid	bend	422	none	none
ivarsson20062 32	F	18015	12.9	PA	mid	bend	364	none	none
ivarsson20062 33	F	19092	13.5	PA	mid	bend	440	none	none
ivarsson20045 34	M	21142	13.6	AP	mid	bend	238	none	none
ivarsson20045 35	M	18884	13.4	PA	mid	bend	381	none	none
ivarsson20049 36	M	29960	14.9	AP	mid	bend	433	none	none
ivarsson20051 37	M	27671	14.8	PA	mid	bend	343	none	none
ivarsson20057 38	F	12172	12	AP	mid	bend	193	none	none

Appendix D: Analyzed Data

Pearson Correlation C	p-value
Age_Ixx	0.0537
Age_mfx	-0.3049
Age_MPS100	-0.5115
Cmax_mfx	0.3228
Cmax_MPS100	-0.1018
Csa_mfx	0.7412
Csa_MPS100	-0.0332
Ixx_mfx	0.5840
Ixx_MPS100	-0.2176
Mass_mfx	0.5085
Mass_MPS100	0.0400
Smod_mfx	0.5753
Smod_MPS100	-0.2091

Age:

Cmax:

Csa:

Ixx:

Mass:

Secmod:

Test configuration:

Loading direction:

Flesh:

Gender:

Location of impact:

Typ of loading:

Impactor velocity:

[CM1]erseten

[CM2]Paper Jeremie

Acknowledgements

Lorem ipsum dolor sit amet, consectetur adipiscing elit. Cras egestas auctor molestie. In hac habitasse platea dictumst. Duis turpis tellus, scelerisque sit amet lectus ut, ultricies cursus enim. Integer fringilla a elit at fringilla. Lorem ipsum dolor sit amet, consectetur adipiscing elit. Nulla congue consequat consectetur. Duis ac mi ultricies, mollis ipsum nec, porta est.

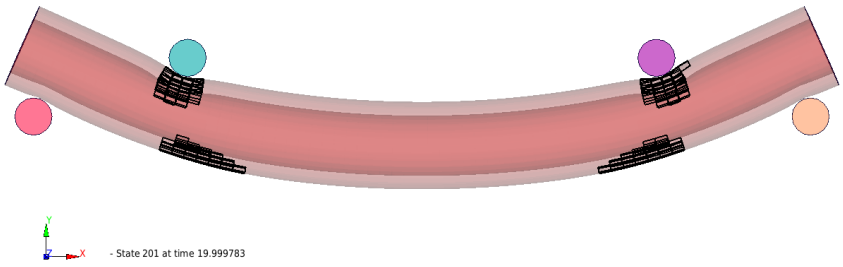

Figure 2: This is a caption